BMC Plant Biology

RESEARCH Open Access

Genome-wide identification of *Morus notabilis* Aquaporin gene family and differential expression of plasma membrane intrinsic proteins in response to *Ralstonia pseudosolanacearum* infection

Siyi Wang[1], Xue Dai[1], Qingqing Tang[1], Jianhao Ding[1], Huicong Shi[1], Weihong Zhou[1,2], Sheng Sheng[1,2] and Ping Li[1,2*]

Abstract

Background Aquaporins (AQPs) play crucial roles in plant water transport, growth and development, and response to biotic and abiotic stresses. Despite their essential functions, the role of AQPs in mulberry trees (*Morus* L.) during *Ralstonia pseudosolanacearum* infection remains largely unknown.

Results In this study, we performed a genome-wide identification and comprehensive characterization of *AQP* genes in *Morus notabilis*. A total of 26 *AQP* genes were identified and classified into four subfamilies: NIP, PIP, SIP and TIP. Furthermore, detailed analyses were conducted on gene structures, protein physicochemical properties, transmembrane domains, phylogenetic relationships, and subcellular localization. Cis-acting element analysis showed that *MnAQP* genes were mainly involved in hormone, light and stress response. Tissue-specific expression analysis demonstrated that the *PIP1* subfamily displayed significantly higher transcript abundance in root tissues relative to leaves, while the *PIP2* subfamily maintained relatively stable expression patterns across various tissue types. In addition, following *R. pseudosolanacearum* inoculation, the expression levels of *PIP* genes were significantly upregulated in the roots, stems, and leaves of mulberry seedlings. These findings indicate that *MnPIP* genes play a crucial role in responding to *R. pseudosolanacearum* infection.

Conclusions This study provides the comprehensive characterization of the *AQP* gene family in mulberry, clarifying the composition and diversity. Our findings establish a solid foundation for further understanding the function roles of *MnPIPs* following *R. pseudosolanacearum* infection in mulberry trees.

Clinical trial number Not applicable.

Keywords Aquaporin, Genome-wide identification, Mulberry, Plasma membrane intrinsic protein (PIP), *Ralstonia pseudosolanacearum*, Gene expression

*Correspondence:
Ping Li
lee_ping2020@163.com
[1]Jiangsu Key Laboratory of Sericultural Biology and Biotechnology, School of Biotechnology, Jiangsu University of Science and Technology, Zhenjiang 212100, China
[2]Key Laboratory of Silkworm and Mulberry Genetic Improvement, Ministry of Agriculture and Rural Affairs, The Sericultural Research Institute, Chinese Academy of Agricultural Sciences, Zhenjiang 212100, China

Introduction

Mulberry (*Morus* spp.), a perennial woody plant widespread across Asia, Africa, and Europe, is of significant economic and ecological value due to its role as the primary food source for silkworms and its nutritional and medicinal properties [1–3]. However, mulberry tree cultivation faces a growing threat from bacterial wilt, a devastating vascular disease caused by the pathogen *Ralstonia pseudosolanacearum* [4]. It has been widely spread through rapid xylem colonization and systemic water conduction disruption in mulberry-planting areas, seriously affecting the development of the sericulture industry, which has inflicted significant losses on the sericulture industry.

Aquaporins (AQPs), a family of small membrane-integrated proteins within the major intrinsic protein (MIP) superfamily, are essential for mediating the transmembrane transport of water and small solutes, such as glycerol, boron, and CO_2 [5]. These proteins demonstrate ubiquitous distribution across major biological taxa, including humans, animals, plants, fungi, and bacteria. AQPs typical form tetramers, each monomer containing six transmembrane domains (TM1-TM6) and five connecting loops LA, LC, and LE on the outer membrane surface and LB and LD on the inner surface [6]. Two helical regions (HB and HE) within the loops extend into the membrane, forming the aqueous pore, which includes highly conserved Asn-Pro-Ala (NPA) motifs in loops B and E [7]. In plants, AQPs are categorized into seven subfamilies: plasma membrane intrinsic proteins (PIPs), tonoplast intrinsic proteins (TIPs), NOD26-like intrinsic proteins (NIPs), X intrinsic proteins (XIPs), hybrid intrinsic proteins (HIPs), small basic intrinsic proteins (SIPs), and GlpF-like intrinsic proteins (GIPs). GIPs and HIPs are exclusive to mosses, ferns, and algae [8, 9]. The number of AQPs varies among species, ranging from 35 in *Arabidopsis thaliana* [10, 11], 33 in rice (*Oryza sativa* L.) [12], 39 in cucumber (*Cucumis sativus* L.) [5], 29 in *Vitis vinifera* [13], 55 in *Populus trichocarpa* [14], and 71 in upland cotton (*Gossypium hirsutum* L.) [15]. Despite their functional importance, AQPs in mulberry remain poorly characterized. The availability of the *Morus notabilis* draft genome [16] provides a valuable resource for exploring the evolution and functional diversity of AQPs in mulberry.

Numerous studies have highlighted the pivotal role of the PIP subfamily in regulating water and solute transport, which significantly influences plant growth, development, and stress responses [17]. Bacterial wilt, caused by *R. pseudosolanacearum*, is characterized by vascular occlusion and water deficiency. The pathogen invades host plants through root tissues, colonizes the xylem, and produces exopolysaccharides (EPS), leading to vessel blockage and subsequent wilting [18–21]. As key regulators of water homeostasis and stress responses, PIPs play crucial roles in plant development and pathogen interactions. However, their specific functions in mulberry during *R. pseudosolanacearum* infection remain largely unexplored. Given the significant threat bacterial wilt poses to mulberry cultivation and the sericulture industry, a comprehensive genome-wide identification of *AQP* genes is essential to elucidate their roles in pathogen response.

This study systematically characterizes the aquaporin (AQP) gene family in mulberry, focusing on tissue-specific and infection-responsive expression dynamics of plasma membrane intrinsic proteins (PIPs) during *R. pseudosolanacearum* pathogenesis. These findings aim to provide critical insights into the functional roles of *PIP* genes in mulberry-pathogen interactions, laying a foundation for future research and potential applications in disease resistance breeding.

Results

Identification and classification of Aquaporin genes in mulberry

Sequence homology analysis and protein domain validation using Pfam identified 26 *AQP* genes in mulberry (Table 1). The HMMER method was employed to search the mulberry database, resulting in the identification of 37 potential AQP sequences. After removing redundancy, a total of 26 distinct AQPs were identified, comprising 10 NIPs, 6 PIPs, 2 SIPs, and 8 TIPs, fewer than the 35 AQPs identified in *A. thaliana*. The fundamental properties of these 26 mulberry AQPs were subsequently analyzed, encompassing coding sequence (CDS) length, protein length, molecular weight, isoelectric point, instability index, aliphatic index, transmembrane domains (TMD), and subcellular localization. The CDS lengths of mulberry *AQP* genes range from 708 (*MnSIP2;1*) to 903 base pairs (bp) (*MnNIP2;3*), putatively encoding proteins of 235–300 amino acids (AA) with molecular weights (MW) vary from 24.9 to 31.98 kilodalton (kDa) and the predicted isoelectric points range from 5.07 to 9.7 (Table 1). Except for MnTIP5;1, all the AQPs were found to be stable. Structural analysis showed that nearly all identified AQPs contain six transmembrane domains, except for MnNIP2;3, which contains only five. Subcellular localization was predicted using Plant-mPLoc. Prediction results showed that the NIP, PIP, and SIP families are all localized to the plasma membrane, with MnSIP2;1 potentially also localizing to the vacuole. Conversely, the TIP family is predominantly localized to the vacuole, with MnTIP5;1 possibly also found in the plasma membrane.

Phylogenetic analysis of Aquaporins in mulberry

To elucidate the taxonomic and evolutionary relationships within the AQP family in mulberry, a neighbor-joining (NJ) phylogenetic tree was constructed using multiple sequence alignments of 90 AQP protein sequences. These sequences included known AQPs

Table 1 List of 26 Aquaporin genes identified in mulberry

Subgroup	Name	CDS length	Protein Length (aa)	[a] MW	[b] pI	Instability index	[c] AI	[d] TM	Predicted location(s)
NIP	*MnNIP1;1*	810	269	28.71	8.33	31.3	113.09	6	Cell membrane
	MnNIP1;2	828	275	29.22	8.75	23.46	103.85	6	Cell membrane
	MnNIP1;3	822	273	29.17	8.81	44.71	113.85	6	Cell membrane
	MnNIP2;1	900	299	31.98	7.12	25.55	97.79	6	Cell membrane
	MnNIP2;2	870	289	30.54	9.7	39.82	95.22	6	Cell membrane
	MnNIP2;3	903	300	31.91	9.42	36.71	97.9	5	Cell membrane
	MnNIP4;1	825	274	28.87	6.06	25.08	104.93	6	Cell membrane
	MnNIP5;1	723	240	25.28	6.74	24.81	98	6	Cell membrane
	MnNIP6;1	759	252	26.16	68.6	23.7	103.81	6	Cell membrane
	MnNIP7;1	711	236	24.9	7.75	20.22	107.08	6	Cell membrane
PIP	*MnPIP1;1*	867	288	30.86	8.79	27.01	97.6	6	Cell membrane
	MnPIP1;2	858	285	30.48	8.3	30.06	99.65	6	Cell membrane
	MnPIP1;3	864	287	30.7	8.9	27.66	97.28	6	Cell membrane
	MnPIP2;1	864	287	30.45	8.45	31.11	107.42	6	Cell membrane
	MnPIP2;2	861	286	30.27	7.03	29.4	97.66	6	Cell membrane
	MnPIP2;7	846	281	30.12	6.64	36.07	103.17	6	Cell membrane
SIP	*MnSIP1;1*	723	240	25.7	9.3	29.33	106.88	6	Cell membrane
	MnSIP2;1	708	235	25.75	9.45	31.67	117.36	6	Cell membrane, Vacuole
TIP	*MnTIP1;1*	756	251	25.87	6.02	23.98	114.7	6	Vacuole
	MnTIP1;2	759	252	25.88	5.14	24.89	110.44	6	Vacuole
	MnTIP1;3	759	252	25.99	5.17	19.1	105.04	6	Vacuole
	MnTIP2;1	747	248	25.18	5.86	23.31	116.09	6	Vacuole
	MnTIP2;2	753	250	25.06	5.07	24.19	121.44	6	Vacuole
	MnTIP3;2	777	258	27.53	6.79	35.63	111.98	6	Vacuole
	MnTIP4;1	753	250	26.38	6.01	27.13	114.72	6	Vacuole
	MnTIP5;1	753	250	25.7	5.83	44.25	105.44	6	Cell membrane, Vacuole

[a] *MW*: Protein Molecular Weight (kDa)

[b] *pI*: Isoelectric Point

[c] *AI*: Aliphatic Index

[d] *TM*: the numbers of transmembrane helices predicted by TMHMM Server v.2.0 tool

from *A. thaliana*, *V. vinifera* and *C. sinensis*, along with those identified in mulberry. The resulting phylogenetic tree showed four distinct clusters representing different classes of AQPs (Fig. 1). The mulberry AQPs were classified according to their clustering with known AQPs from other species and categorized into 6 MnPIPs, 8 MnTIPs, 10 MnNIPs and 2 MnSIPs. The 26 candidate sequences identified in mulberry were found to exhibit high similarity to corresponding subfamilies in other plants and were clustered closely within the same groups. Within the mulberry AQPs groups, two major MnPIP subgroups, MnPIP1 and MnPIP2, each comprising three members, were observed. It was noteworthy that the number of PIP family members in mulberry was found to be fewer than in *Arabidopsis.* The NIP subfamily was identified as the most abundant in mulberry, while the SIP subfamily was the least represented.

Characterization of conserved motifs and domains in mulberry Aquaporins

Multiple sequence alignment showed that MnAQPs have a close homologous evolutionary relationship (Fig. 2A). To further investigate sequence characteristics and evolutionary relationships among subfamilies, we performed conserved motifs using MEME (26 AQP members), analyzed structural domains via NCBI-Conserved Domain Database, and visualized results using TBtools. Comprehensive sequence analysis identified 12 conserved motifs (motifs 1–12) and three key structural domains (PLN00027, MIP, and MIP superfamily) in the aquaporin family. Phylogenetic analysis revealed universal conservation of motifs 1–5 across all subfamilies (Fig. 2B), indicating their essential role in maintaining structural integrity during evolution. Subfamily-specific analysis further highlighted distinct structural features among subgroups. Notably, the TIP subfamily uniquely exhibited motifs 14 and 15, absent in other subfamilies, while retaining both the PLN00027 and MIP superfamily domains (Fig. 2C). Furthermore, All PIP subfamily members retained a core set of conserved motifs (7, 8, and 11), with PIP1 isoforms specifically containing an additional motif 9 compared to PIP2 isoforms, while maintaining the MIP domain. The NIP subfamily

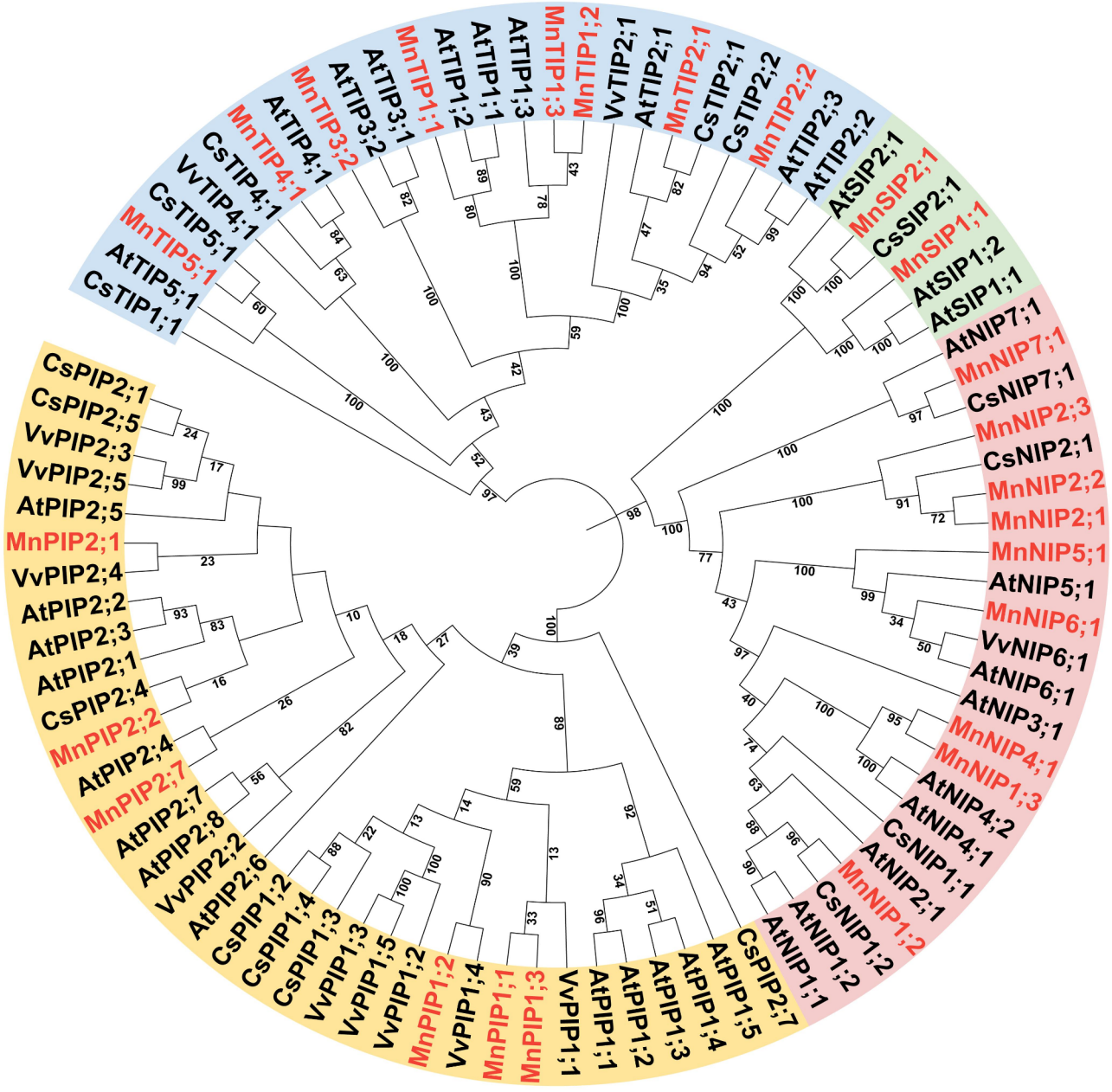

Fig. 1 Phylogenetic relationships of AQP family in *A. thaliana*, *C. sinensis*, *V. Vinifera* and *M. notabilis*. The AQP protein sequences were aligned by Clustal W and the phylogenetic tree was constructed in MEGA X based on the Neighbor-Joining (NJ) method with the results of 1000 bootstrap replications. The yellow, pink, green, and blue colors represent the PIP, NIP, SIP, and TIP subfamilies of aquaporins, respectively

exhibited distinct combination of motifs (10, 12, and 13) together with the MIP superfamily domain. In contrast, the SIP subfamily displayed the most simplified domain, retaining solely the MIP superfamily domain but with an atypical structural arrangement. The observed structural heterogeneity provides critical molecular evidence for the functional divergence of aquaporin subfamilies, offering new insights into their distinctive roles in transmembrane transport and cellular homeostasis.

Analysis of cis-acting regulatory elements of *MnAQP* genes

Cis-acting regulatory elements interact with specific transcription factors to modulate gene transcription. To investigate the potential functions of *MnAQP* genes and their responses to various signaling factors, we employed the PlantCARE database to predict cis-acting elements within the putative promoter regions of *MnAQP* genes [22]. A total of 92 distinct cis-acting elements were identified, exhibiting significant variations in roles and regulatory mechanisms. Our analysis focused on hormone

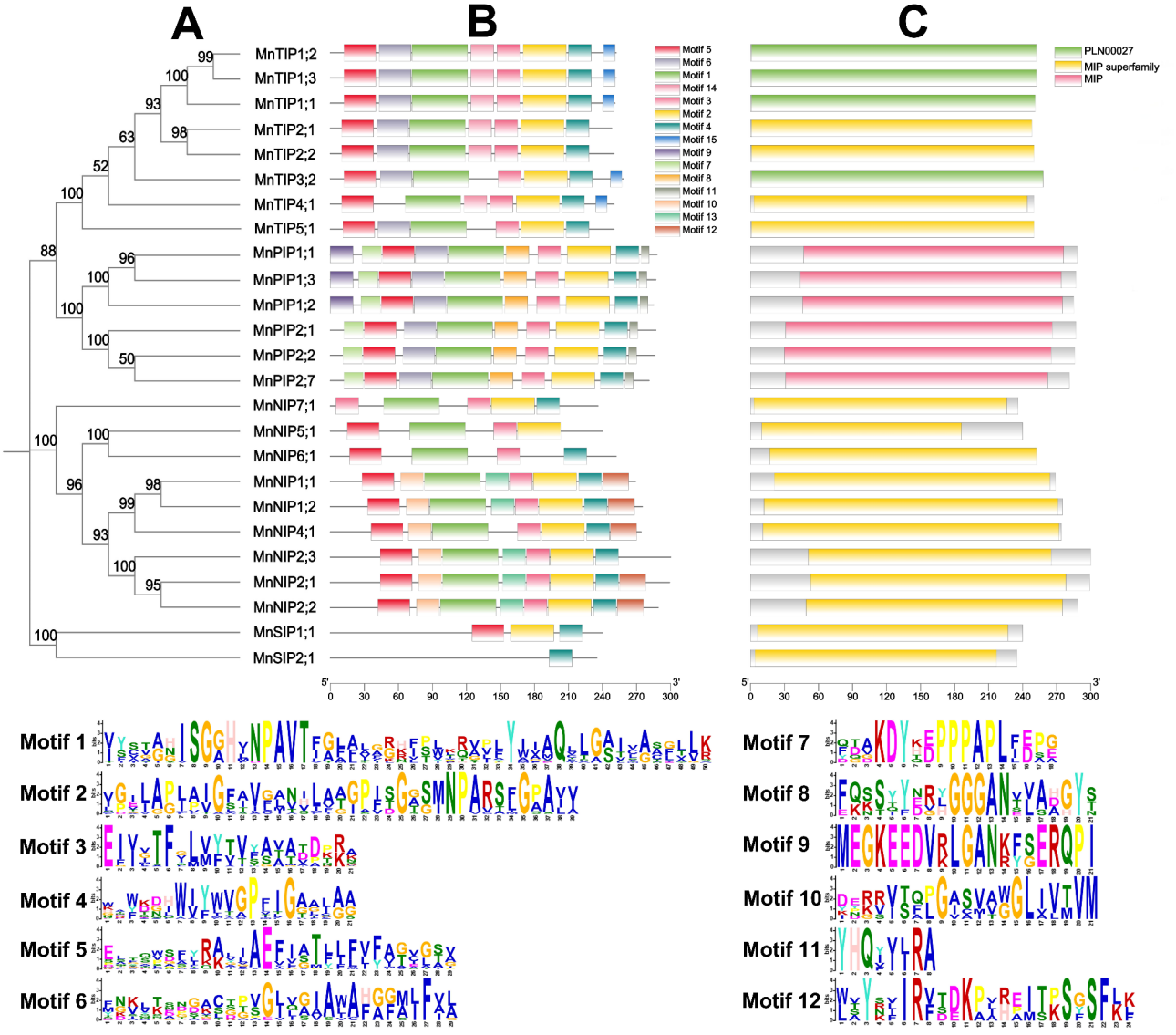

Fig. 2 Conservation analysis of motifs and domains in mulberry aquaporins. (**A**) Neighbor-Joining (NJ)-based phylogenetic tree of mulberry aquaporin (AQP) proteins; (**B**) Identification of conserved motif of MnAQP proteins by MEME suite. Different colored boxes indicate different motif types. (**C**) Conserved domains of MnAQP proteins. Different colored boxes indicated different domains

response, light response, stress response, and plant growth-related elements. Key hormone-responsive elements included ABRE (ABA-responsive), TCA-element (SA-responsive), ERE (Ethylene-responsive), GARE-motif, P-box, and TATC-box (gibberellin-responsive), CGTCA-motif and TGACG-motif (MeJA-responsive), and TGA-element (auxin-responsive) (Fig. 3A). Light-responsive elements comprised G-box, GATA-motif, I-box, TCT-motif, AE-box, GT1-motif, and Box 4 (Fig. 3A). Stress-responsive elements including TC-rich repeats, MBS (MYB binding site involved in drought-inducibility), MYC, Myb, Box S, W-box, LTR (low-temperature responsive) and WUN-motif (wound-responsive) (Fig. 3A). Additionally, we identified elements related to plant growth: GCN4-motif (endosperm expression), CAT-box (meristem expression), and O_2-site (zein metabolism regulation) (Fig. 3A). Most identified cis-acting elements were associated with hormone response, light response, and stress response (Fig. 3B), suggesting that *MnAQP* genes may play roles in responding to both biotic and abiotic stresses. However, further experimental validation is needed to confirm these findings and elucidate the precise regulatory mechanisms under various environmental conditions.

Prediction of secondary and tertiary structure of MnPIP1;2 in mulberry

Plasma membrane intrinsic proteins represent the largest subfamily of plant AQPs [23] and serve as the major channels for maintaining water homeostasis [24].

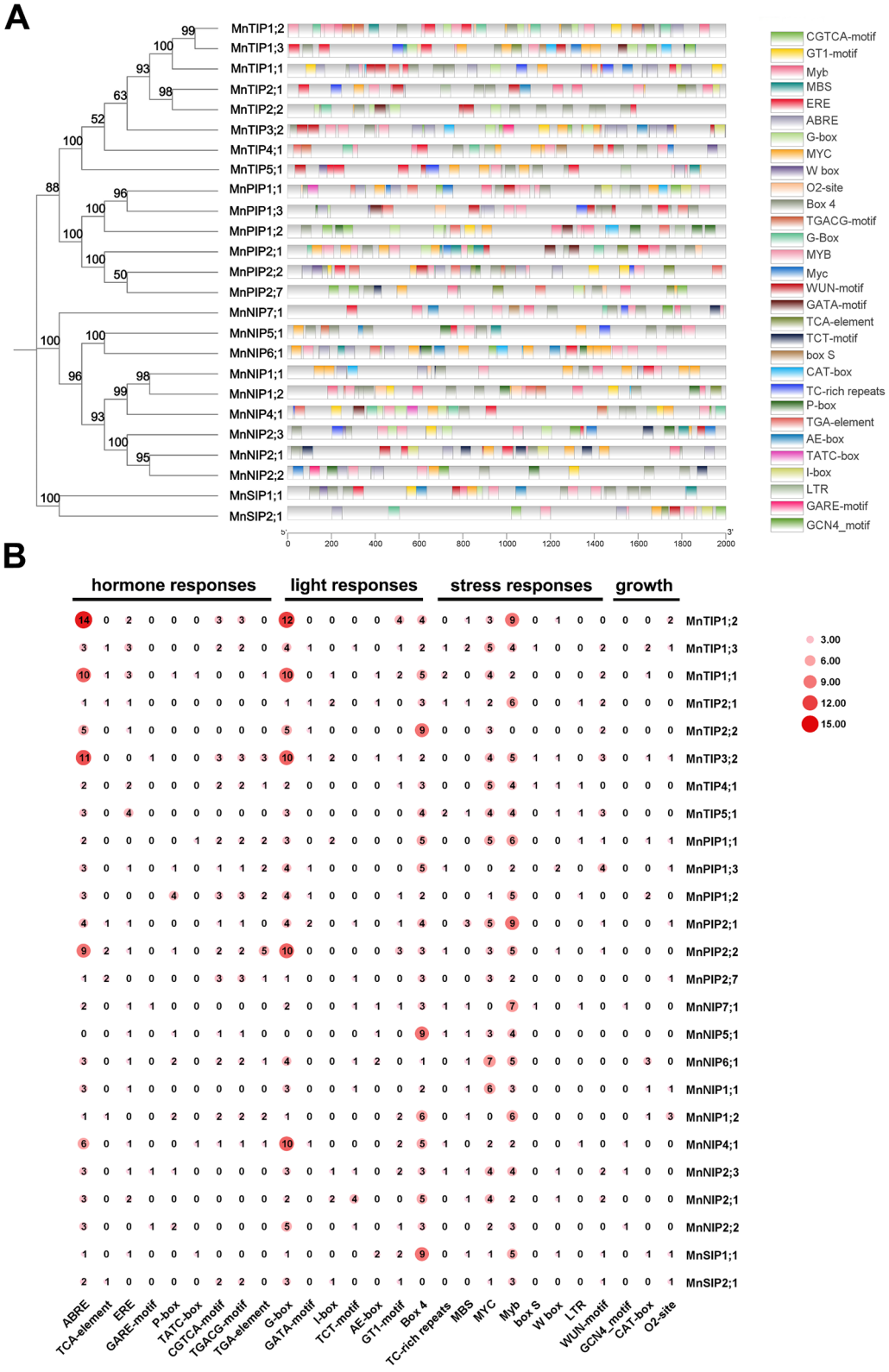

Fig. 3 The cis-acting elements analysis of putative promoter regions of *MnAQP* genes. (**A**) Localization of cis-acting elements within the 2 kb upstream sequence of *MnAQP* genes. Distinct cis-acting elements are color-coded for visual differentiation, with each color corresponding to a specific type of regulatory element. (**B**) Heatmap representation of the predicted cis-acting elements in the *MnAQP* promoter region. The heatmap illustrates the quantitative distribution of these elements, with numerical annotations indicating the frequency of each cis-acting element type

Numerous studies have highlighted their crucial role in facilitating plant growth, development, and resistance to both biotic and abiotic stresses. Given the limited research on the PIP family in mulberry, this subfamily was selected for detailed investigation. Taking MnPIP1;2 as an example, CDD analysis revealed that this protein contains a highly conserved MIP domain, characteristic of the AQP family. This domain, consisting of 231 amino acid residues located between positions 46 and 276 (Fig. 4A), represents the typical features of the AQP family. SOPMA analysis indicated that the secondary structure of MnPIP1;2 consists of 32.63% α-helices, with no β-bridge, 16.84% extended strands, and 50.53% random coils. The overall secondary structure is predominantly composed of α-helices and random coils (Fig. 4B). TMHMM predictions revealed six potential α-helical transmembrane segments in MnPIP1;2, located at residues 55–75, 91–110, 135–155, 180–198, 211–231, and 258–279, with lengths of 21, 20, 21, 19, 21, and 22 residues, respectively (Fig. 4C). Further confirmation using AlphaFold 3D homology modeling demonstrated that the protein contains six transmembrane helices and can potentially form a homotetramer (Fig. 4D). Additionally, multiple sequence alignment of the six MnPIPs annotated conserved NPA (Asn-Pro-Ala) motifs in the transmembrane domains (TM1-TM6) and two half-helices (HB and HE) (Fig. 4E). These findings establish a theoretical foundation for studying the structure and function of the mulberry PIP family, highlighting the importance of MnPIP1;2 in water transport and stress resistance mechanisms.

Subcellular localization analysis of the pips in mulberry

The plasma membrane is the primary site for AQP localization and plays a crucial role in maintaining cellular water homeostasis, supporting normal physiological processes. Therefore, the plasma membrane localization of the PIP family is vital to its function. According to bioinformatic predictions using Plant-mPLoc, all MnPIP proteins were localized to the plasma membrane. To further verify the subcellular localization of MnPIPs, the enhanced green fluorescent protein (eGFP) was fused to the N-terminus of *MnPIP1;1*, *MnPIP1;2*, *MnPIP1;3*, *MnPIP2;2* and *MnPIP2;7*, respectively. The subcellular localization of these fusion proteins was analyzed using confocal laser scanning microscopy following transient expression in tobacco leaves. Expression of eGFP alone exhibited characteristic cytoplasmic and nuclear staining, whereas all eGFP-MnPIPs fusion proteins localized specifically to the plasma membrane (Fig. 5), consistent with our previous bioinformatics predictions. Notably, the eGFP-MnPIP1;3 fusion protein displayed distinct movement at the cell membrane (Supplementary material 2). Due to the failure in cloning the *MnPIP2;1* gene, its subcellular localization was not experimentally determined in this study. Nevertheless, prior prediction using the Plant-PLoc online tool indicated that MnPIP2;1 is likely localized to the plasma membrane (Table 1). In summary, these findings confirm that the plasma membrane is likely the primary site where MnPIPs proteins exert their biological functions.

Expression analyses of the *MnPIP* genes in mulberry tree of different tissues

To further investigate the potential functions of *MnPIPs* in mulberry tree growth and development, RT-qPCR analysis was performed to examine the expression of six *MnPIP* genes across roots, stems and leaves (Fig. 6). The expression profiles of these genes varied significantly among different tissues. The *MnPIP1;1*, and *MnPIP1;3* were high expressed in roots (Fig. 6A), *MnPIP1;3*, *MnPIP2;7* were most highly expressed in stems (Fig. 6B), and *MnPIP1;3* were higher expression in leaves compared to other members of the *MnPIP* family (Fig. 6C). Conversely, *MnPIP1;2*, *MnPIP2;1* and *MnPIP2;2* were found to have low expression levels across all three tested tissues (Fig. 6). Notably, it was exhibited that the expression of the *MnPIP1* subfamily demonstrated tissue specificity, being predominantly concentrated in the roots. In contrast, the *MnPIP2* subfamily showed relatively consistent expression levels across different tissues. The constant expression in all tissues indicated that PIPs play a crucial role in mulberry physiology, suggesting that these proteins might have distinct functions concerning development and defense mechanisms against adverse conditions.

Expression profiling of *PIP* genes in response to *R. pseudosolanacearum* infection in mulberry

Bacterial wilt, caused by *R. pseudosolanacearum*, is a major soil-borne bacterial disease of mulberry that severely limits the sustainable development of the sericulture industry [25]. Previous studies have suggested that the *PIP* gene family may play a role in plant responses to bacterial, fungal and viral infections [26–28], yet it remains unclear whether mulberry *PIP* genes respond to *R. pseudosolanacearum* infection. To investigate the expression patterns of *PIP* genes in different mulberry tissues following infection with *R. pseudosolanacearum*, RT-qPCR was used to quantify the expression levels of *PIP* genes at 0, 6, 12, 24, 48, 72 and 96 h post-infection. The results indicated that *R. pseudosolanacearum* infection induced the expression of *PIP* genes in various mulberry tissues. In the root it was found that five *PIP* genes (*PIP1;1*, *PIP1;3*, *PIP2;1*, *PIP2;2*, and *PIP2;7*) were significantly up-regulated 12 h post-infection with *R. pseudosolanacearum*, while *PIP1;2* showed noticeable up-regulation at 6 hpi, suggesting a quicker response

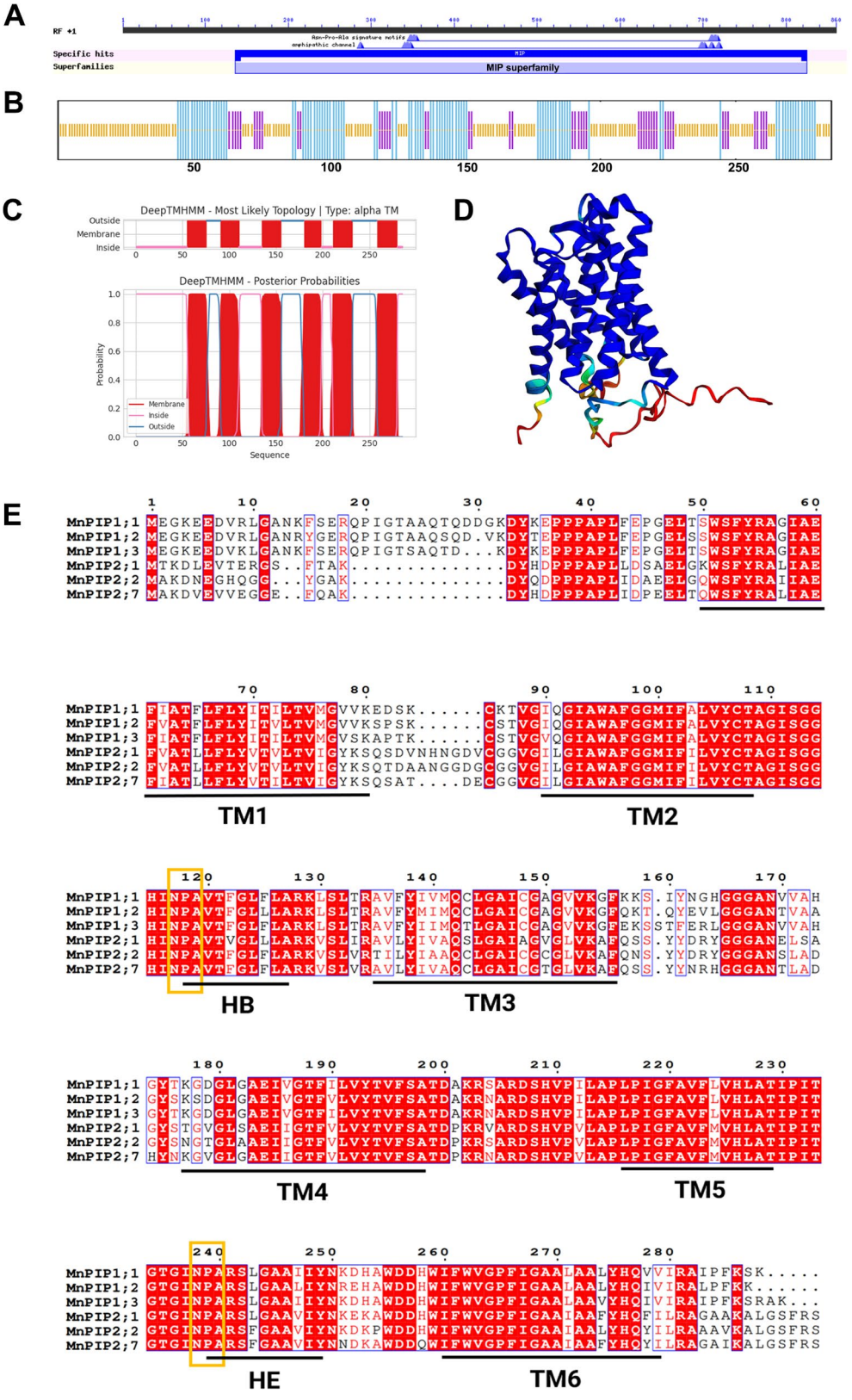

Fig. 4 Bioinformatics analysis of MnPIP1;2. (**A**) Domain analysis of MIP superfamily; (**B**) Secondary domain analysis of MnPIP1;2; (**C**) Transmembrane domain analysis of MnPIP1;2; (**D**) Prediction of the tertiary structure of MnPIP1;2; (**E**) Alignment of the amino acid sequence of MnPIP1;2. TM1-TM6: Represent six distinct transmembrane domains. HB and HE: Two half-helical regions. Yellow Frame: Highlights the conserved NPA (Asn-Pro-Ala) motifs

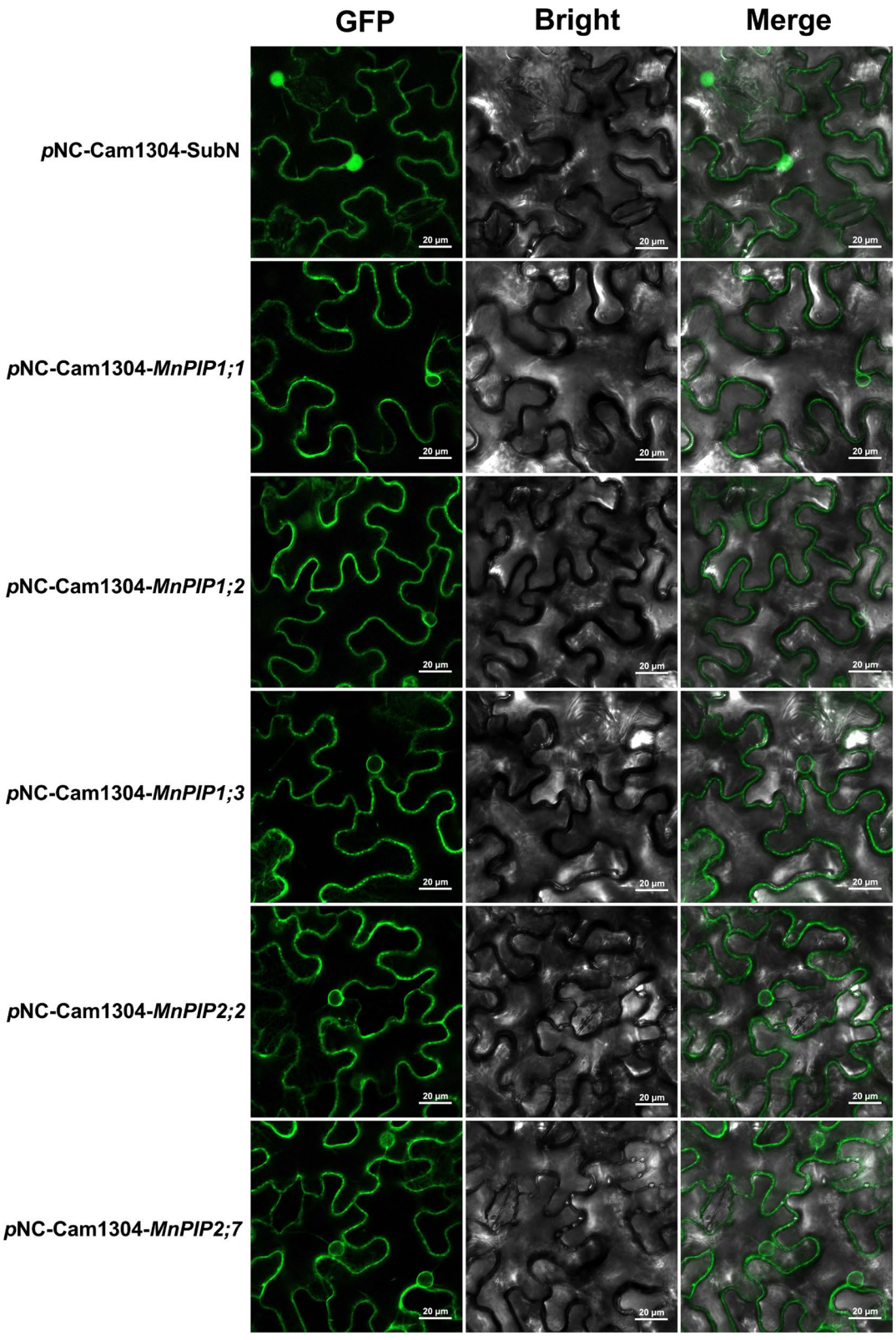

Fig. 5 The subcellular localization of MnPIPs. The empty vector *p*NC-Cam1304-SubN as a negative control. After 48 h of *Agrobacterium* infiltration, transient expression analysis was performed using *PIPs*-GFP fusion constructs in *Nicotiana benthamiana* leaves. Scale bars = 20 μm

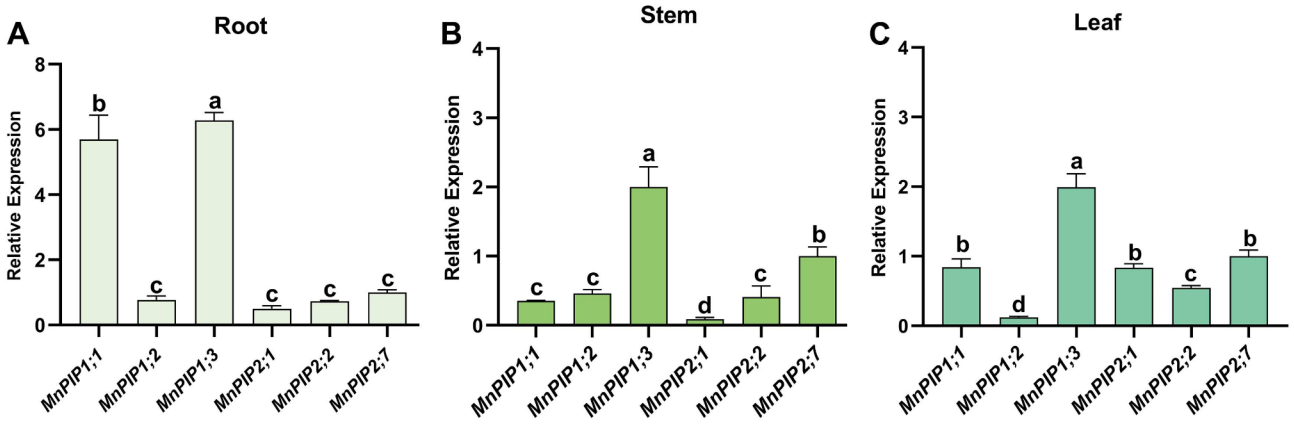

Fig. 6 Analysis of different tissues (root, stem and leaf) expression patterns of *MnPIPs*. (**A**) Expression patterns of six *MnPIP* genes in mulberry root tissue; (**B**) Expression patterns of six *MnPIP* genes in mulberry stem tissue; (**C**) Expression patterns of six *MnPIP* genes in mulberry leaf tissue. Three biological replicates were performed and error bars are means ± standard deviation (SD). Differences in the expression levels of each target were compared using one-way analysis of variance (ANOVA) with Tukey's *post hoc* test. The letters above the error bars indicate significant differences among different samples (least significant difference, $P < 0.05$)

than other *PIP* genes (Fig. 7). Additionally, *PIP1;2*, *PIP1;3*, and *PIP2;2* reached their highest expression levels at 48 hpi (Fig. 7B, C, E), whereas *PIP2;1* and *PIP2;7* peaked at 96 hpi (Fig. 7D, F). Notably, the degree of up-regulation varied considerably among the *PIP* genes, with the *PIP2* subfamily showing ranged from 3 to 7-fold, while the up-regulation of the *PIP1* subfamily varied significantly, ranging from 2 to 30-fold increases. Among these, *PIP1;2* exhibited the highest level of up-regulation, with its expression increasing by more than 30-fold at 48 hpi. In the stem (Fig. 8), with the exception for *PIP1;1*, which was up-regulated at 24 hpi, the expression levels of the other *PIP* genes were higher than those of the control group at 6 hpi. This indicated that the *PIP* genes in the stem were more rapidly up-regulated in response to *R. pseudosolanacearum* infection compared to those in the root. Notably, the up-regulation of *PIP* genes in the stem was found to be less pronounced than that in the root. However, *PIP1;2* was up-regulated by 15-fold at 96 hpi in the stem (Fig. 8B), confirming that *MnPIP1;2* exhibits strong differential expression in both root and stem tissues following infection by *R. pseudosolanacearum*, demonstrating a significant response to the bacterial infection. In the leaf (Fig. 9), the *PIP2;1* gene exhibited the first signs of up-regulation at 6 dpi (Fig. 9D), followed by a significant up-regulation of three *PIP* genes (*PIP1;1*, *PIP1;2* and *PIP2;2*) at 12 hpi (Fig. 9A, B, E). In addition, *PIP1;3* and *PIP2;7* were significantly up-regulated at 48 h (Fig. 9C) and 72 h (Fig. 9F), respectively, following infection with *R. pseudosolanacearum*. It is worth noting that the fold change in the expression of *PIP* genes in mulberry leaf tissues was much lower than that in root and stem tissues. The expression of most genes was up-regulated by 1 to 4-fold following bacterial infection. Furthermore, *PIP1;1* and *PIP2;7* were significantly down-regulated at 96 hpi compared to the control group (Fig. 9A, F). In summary, the *PIP* genes in mulberry exhibited varying degrees of upregulation at different time points following *R. pseudosolanacearum* infection, with this trend being more pronounced in the roots and stems than in the leaves. These findings suggest that *PIP* genes play a crucial role in the defense mechanisms against bacterial wilt, particularly in root and stem tissues, where their expression is highly induced in response to infection.

Discussion

High conservation of Aquaporins members in mulberry

Water was recognized as the most important component of any living cell, and aquaporins initially raised considerable interest due to their role as water channels. To date, the *AQP* gene family has been characterized in an increasing number of species, including animals, plants, and microbes. In humans, there are 13 AQPs, designated AQP0 through AQP12, which play crucial roles in cell proliferation and migration, gas permeation, signal transduction, and other physiological functions [29]. Since the discovery of plant aquaporins, an increasing number of aquaporin genes have been reported. Unlike animals, plants exhibit a remarkably diverse set of aquaporin homologues [30]. Recent advancements in genome sequencing and assembly have revealed the distribution and structural characteristics of AQP family members across various plant species [6, 10, 31–35]. Given the limited existing knowledge regarding aquaporins in mulberry, a genome-wide identification of mulberry aquaporins was conducted in this study. A total of 26 AQPs were identified and subsequently classified into four subfamilies: 6 PIPs, 10 NIPs, 8 TIPs, and 2 SIPs. Previous studies have identified 33 AQP family members in *Vitis vinifera*, including 11 PIPs, 8 NIPs,

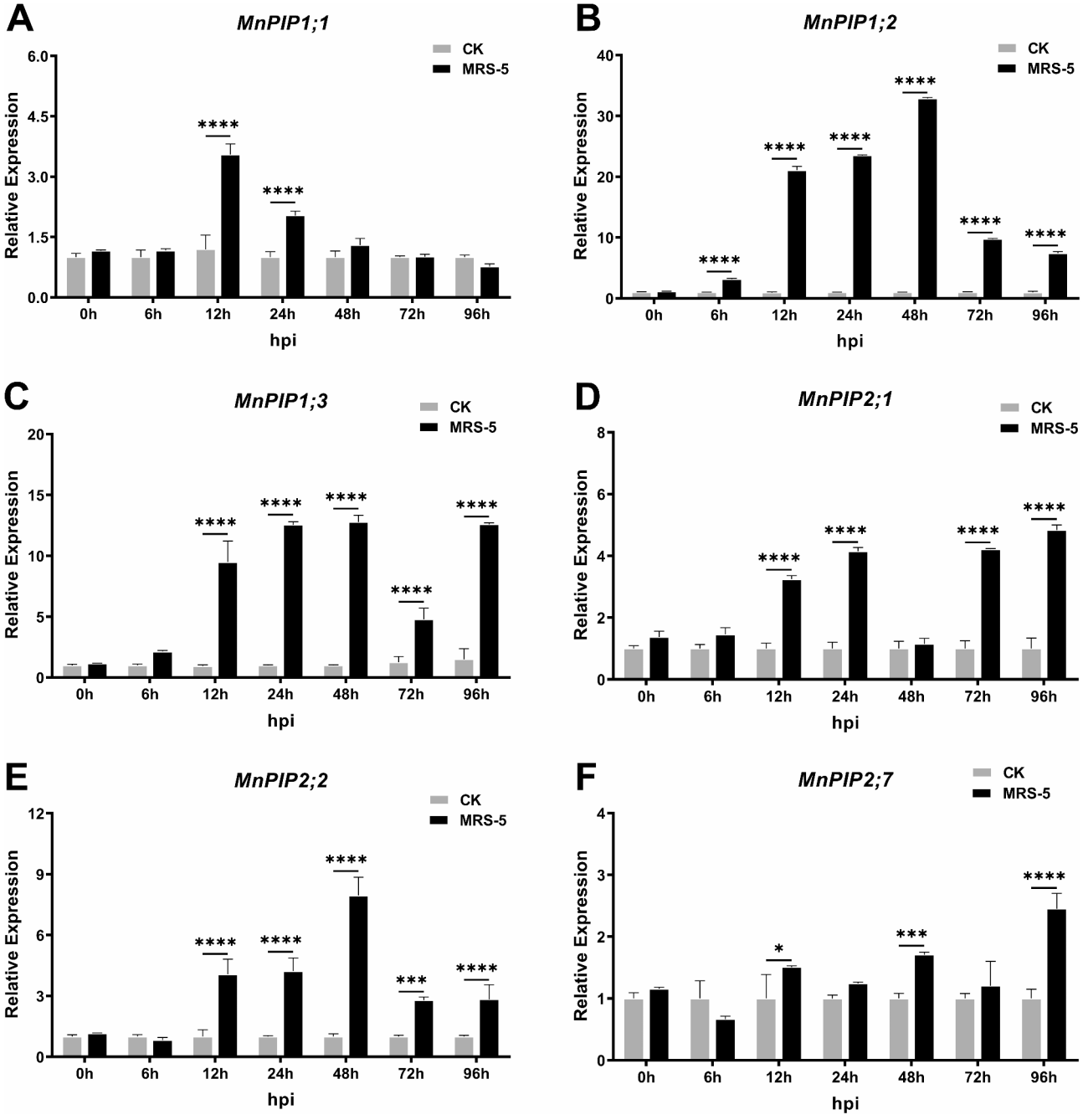

Fig. 7 Expression of *MnPIP* genes in mulberry roots after the infection of *R. pseudosolanacearum*. Differences in the expression levels of each target were compared using Student's *t*-test method. Three biological replicates were performed for each sampling time point, and each biological replicate consisted of multiple individuals. Error bars are means ± standard deviation (SD). Asterisks indicate significant differences between healthy and *R. pseudosolanacearum* treatment groups within the same point (*$P < 0.05$, **$P < 0.01$, ***$P < 0.001$, ****$P < 0.0001$)

11 TIPs, 2 XIPs, and 1 SIP [14]. Similarly, a genome-wide analysis of *Betula pendula*, another woody plant, revealed 33 *AQP* genes, comprising 10 PIPs, 8 TIPs, 8 NIPs, 4 XIPs, and 3 SIPs [36]. The model plants such as *Arabidopsis*, rice and maize contain more than 30 AQPs, which can be divided into at least four subfamilies based on phylogenetic analysis [7, 12, 37]. The total number of AQPs in mulberry is relatively low, with fewer PIP members compared to other plants. Notably, the XIP, GIP and HIP subfamilies were not identified in mulberry, suggesting potential evolutionary loss. While the XIP subfamily is absent in most plant species, it has been reported in some plants like common beans, soybeans, and bay beans. However, XIPs are also absent in

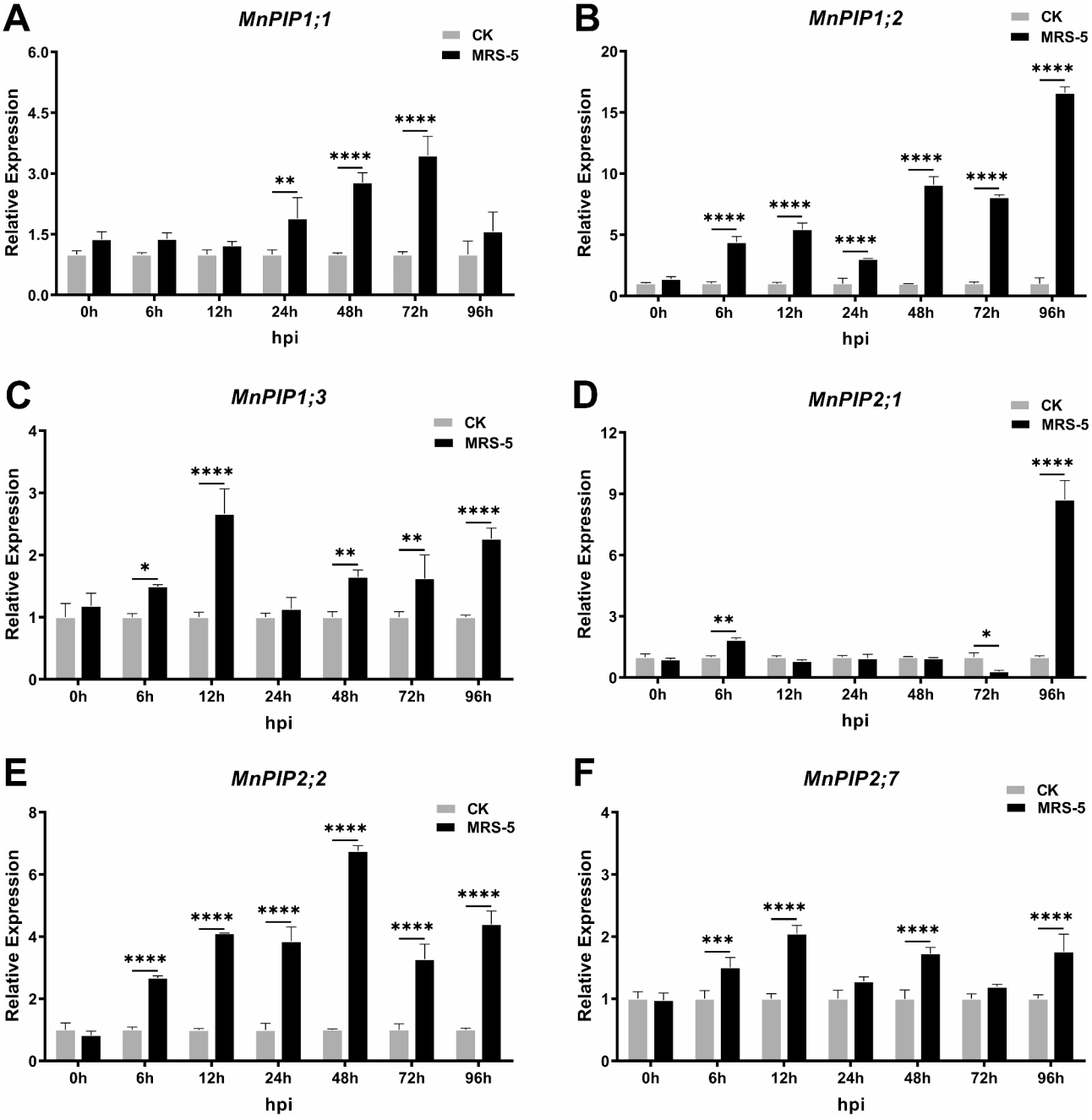

Fig. 8 Expression of *MnPIP* genes in mulberry steams after the infection of *R. pseudosolanacearum*. Differences in the expression levels of each target were compared using Student's *t*-test method. Three biological replicates were performed for each sampling time point, and each biological replicate consisted of multiple individuals. Error bars are means ± standard deviation (SD). Asterisks indicate significant differences between healthy and *R. pseudosolanacearum* treatment groups within the same point (*$P < 0.05$, **$P < 0.01$, ***$P < 0.001$, ****$P < 0.0001$)

crops such as chickpeas and mustard greens, indicating that XIPs may not be essential for critical physiological processes in many species [38]. Many higher plants possess more than 30 AQP members, indicating that the 26 AQPs identified in mulberry might be incomplete and could be missing some members. For instance, only 29 members of the MIP family were initially identified in the grapevine [39], but recent advancements in genome assembly have expanded the number to 33 [13]. Given that the mulberry genome is larger (estimated at 410.45 Mb) than that of *A. thaliana* [40], it is likely that numerous uncharacterized *AQP* genes exist within the mulberry genome. Future research will focus on exploring additional *AQP* genes in mulberry and elucidating their roles in plant growth and development.

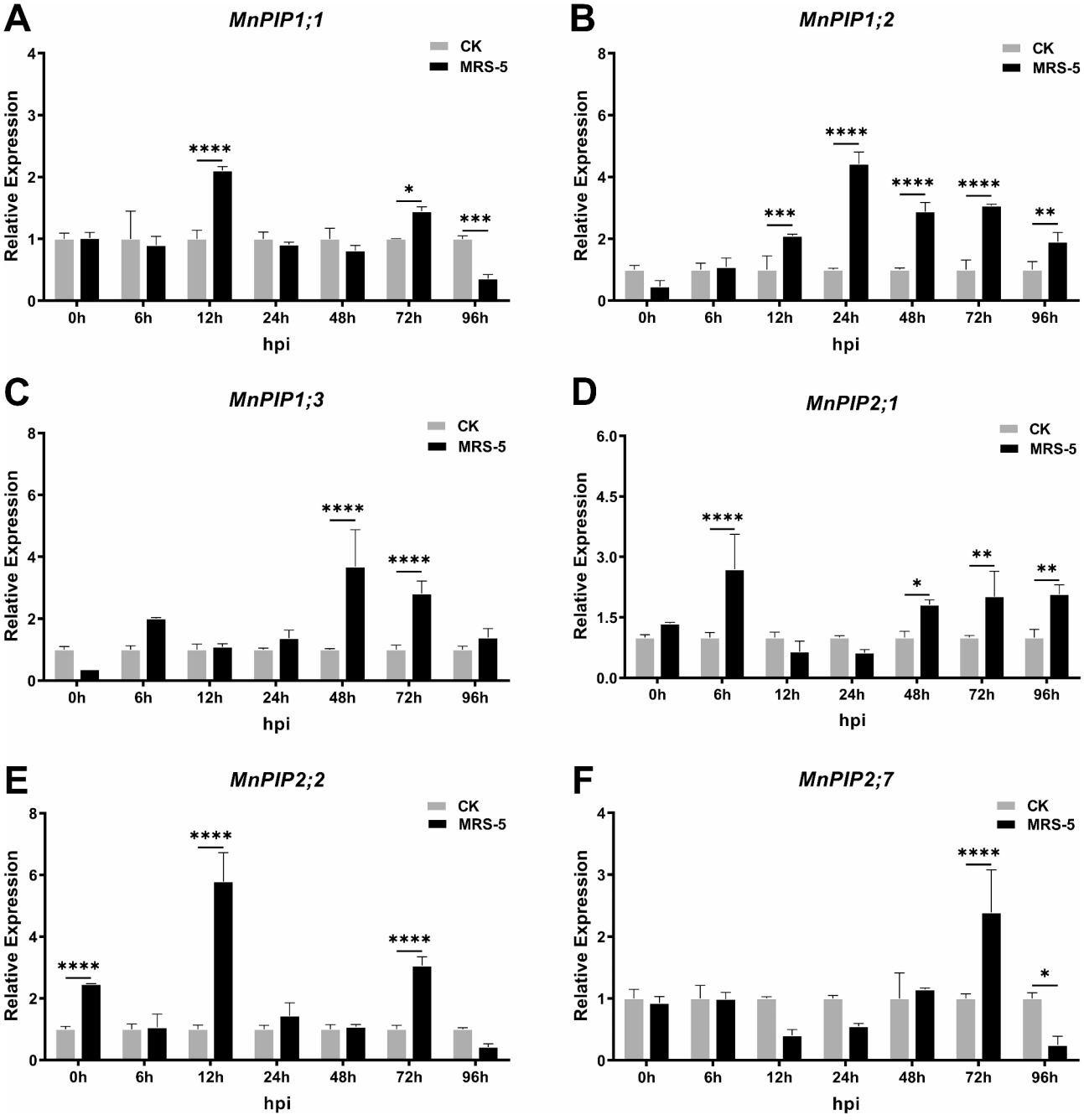

Fig. 9 Expression of *MnPIP* genes in mulberry leaves after the infection of *R. pseudosolanacearum*. Differences in the expression levels of each target were compared using Student's *t*-test method. Three biological replicates were performed for each sampling time point, and each biological replicate consisted of multiple individuals. Error bars are means ± standard deviation (SD). Asterisks indicate significant differences between healthy and *R. pseudosolanacearum* treatment groups within the same point (*$P < 0.05$, **$P < 0.01$, ***$P < 0.001$, ****$P < 0.0001$)

Molecular basis of PIP-dependent pathogen resistance

Research has demonstrated that aquaporins were not merely water-selective channel proteins, they also possessed a variety of physiological and biochemical functions, classifying them as multifunctional proteins. AQPs have been shown to play diverse roles, including regulating plant development and growth and responding to abiotic stresses such as drought, cold, and salinity. Additionally, *AQP* genes may be involved in responding to biotic stresses, including those caused by diseases and insect infestations [32]. The PIPs subfamily is regarded as the primary pathway for water transport across the plasma membrane in root and leaf tissues, playing a crucial role in plant hydric dynamics [41–45]. PIPs possess extracellular regions exposed to the external environment, suggesting their potential involvement in plant

responses to biotic and abiotic stresses [46]. In addition, plant aquaporins not only provide water for each developmental stage, but also participate in regulating of pathogen pathogenicity and the plant immune response [47]. Root PIPs from halophytes were reported to be regulated through clathrin-coated vesicles (CCV) trafficking and phosphorylation. Under salinity conditions, these processes impacted the localization, transport activity, and abundance of PIPs [48]. In rice, OsPIP2;2 was identified as a predominant facilitator of water transport relevant to drought tolerance in plants [49]. It positively regulated plant innate immunity by mediating the transport of H_2O_2 into plant cells and mediating the translocation of OsmaMYB from the plasma membrane to the nucleus [26]. Additionally, OsPIP1;3 interacts with the bacterial translocator Hpa1 at the rice plasma membrane, controlling the translocation of PthXo1 from bacterial blight pathogen cells into the cytosol of susceptible rice variety [50]. Moreover, it was found that AtPIP1;4 and AtPIP2;4 collaborated to transport bacterial pathogens and flg22-induced apoplastic H_2O_2 into the cytoplasm, leading to increased callose deposition and enhanced expression of defense genes, thereby strengthening immunity [51]. A conserved and novel pathway initiated by GP1pro targeted the plant aquaporin protein NbPIP2;4, transporting apoplast-to-cytoplast H_2O_2 to regulate plant immunity [52]. Compared with *Arabidopsis* [53], *Oryza sativa* [49, 50], and *Zea mays* [54], there are few reports on PIPs in mulberry. In *morus*, *MnPIP1;3* was the highest expressed *PIP*, exhibiting high abundance in roots, stems and leaves (Fig. 6). These findings are similar to previous studies on tea plants, where the *CsPIP* subfamily was shown to exhibit higher transcription levels in flowers, roots, and tender stems than in other tissues [55]. In addition, it was reported that all *ZmPIP* genes, except for *ZmPIP2;7*, were expressed in the primary roots of maize [56]. Furthermore, Shinobu Suga et al. also reported that the plasma membrane aquaporins *RsPIP1* and *RsPIP2* accumulated at high levels in the cambium of radishes [57]. The higher expression levels of *PIP* genes in the roots, stems and leaves of mulberry indicate that these proteins serve as key AQPs for water and solute transport in mulberry.

The water transport capability of mulberry PIPs may be related to their protein structure and plasma membrane localization

Studies on the functions of PIPs have also shown that these proteins significantly promote root water uptake. In two allelic *Arabidopsis pip2;2* knockout mutants, a reduction of 25-30% in the hydraulic conductivity of root cortex cells was observed compared to wild-type plants [58]. In higher plants, long-distance transport of liquids is primarily mediated by vascular tissues, which are characterized by the absence of significant membrane barriers. However, during processes such as transpiration or growth expansion, living tissues may experience intense water flow. Consequently, water can move through various pathways: (i) the apoplastic pathway, where it flowed within the continuum of cell walls; (ii) the symplastic pathway via cytoplasmic continuity and plasmodesmata; and (iii) the transcellular pathway, traversing cell membranes—mainly the plasma membrane—where aquaporins played a crucial role in many tissues [44]. Through predictions of the tertiary structure of the MnPIP1;2 protein, it was found that this protein could form a tetramer structure (Fig. 4D). Fluorescence resonance energy transfer (FRET) imaging conducted in living maize protoplasts co-expressing PIP1 and PIP2 proteins, further substantiated a model wherein aquaporins of these two classes engaged in direct interactions, most likely through heterotetramerization, thereby facilitating the trafficking of PIP1 [59]. It remains unknown whether the PIP1 and PIP2 subfamily interact to promote water transport in mulberry. The cellular distribution of some aquaporins appears more complex than simple localization to the plasma membrane or tonoplast. For instance, Maize ZmPIP1;2 and ZmPIP2;5, when fused with GFP, were detected not only on the plasma membrane but also in the inner membrane and perinuclear region, suggesting stages of PIP transport within the secretory pathway [60]. Homologous proteins of *Arabidopsis* plasma membrane PIP1 were found in complex invaginations of the plasma membrane known as plasma membrane bodies, which might promote water exchange between the apoplasts and vacuoles. In this experiment, the subcellular localization of the MnPIPs family was analyzed. The results showed that PIP1;1, PIP1;2, PIP1;3, PIP2;2, and PIP2;7 emitted green fluorescence signals on the plasma membrane of *N. benthamiana*, whereas the fluorescence in the control group was dispersed throughout the tobacco cells. Additionally, it was found that some MnPIP1;3 could move within the cytoplasm, a phenomenon that has not yet been fully explain (Supplementary material 2). It is speculated that the cytoplasmic mobility of MnPIP1;3 may be related to its functional regulation within the cell, potentially involving roles in intracellular signaling, material transport, or other biological processes.

PIP genes in the roots and stems of mulberry can respond to *R. pseudosolanacearum* infection

Most studies on PIPs in plants have focused on gene cloning and expression analysis. However, little is known about the response of PIPs to plant pathogen infection. *Ralstonia solanacearum* can infect more than 400 species of plants in over 50 families, especially affecting Solanaceous plants, such as tomato (*Solanum lycopersicum*), potato (*Solanum tuberosum*) and tobacco (*Nicotiana*

tabacum.). Due to the complexity of mulberry bacterial wilt caused by *R. pseudosolanacearum*, the pathogenesis remains poorly understood, and no effective preventive and control measures had been available in agricultural production. In recent years, losses due to bacterial wilt in mulberry trees have been reduced through the implementation of comprehensive management strategies, including plant quarantine measures and the cultivation of resistant varieties. However, the pathogenic mechanism of mulberry bacterial wilt has not been fully elucidated. Given that bacterial wilt is a typical vascular disease, water transport plays a crucial role in the infection process of *R. pseudosolanacearum* in mulberry. To investigate the expression patterns of *PIP* genes in mulberry plants infected by *R. pseudosolanacearum*, samples were collected at 0 h, 6 h, 12 h, 24 h, 48 h, 72 h and 96 h after inoculation using hydroponic root injury methods (Fig. S1). By comparing the results of RT-qPCR, it was found that *PIPs* genes in different tissues of mulberry were up-regulated following *R. pseudosolanacearum* infection. The expression levels of most genes showed an initial increase followed by a downward trend (Figs. 7, 8 and 9). These results were consistent with the expression patterns of *PIPs* in other plants under pathogen infection. For example, the transcript levels of *TaPIPs* in wheat leaves inoculated with *Blumeria graminis* increased to varying degrees three days post-inoculation compared to the controls. For most genes, the increase was less than two-fold, but the transcripts of *TaPIP2;10* increased by 5.62-fold [61]. Furthermore, after inoculation with the virulent *Phytophthora capsici* HX-9 strain in Pepper cv. P70, the *CaPIP1-1* transcript levels in leaves were upregulated 2-fold compared to the control level at 1 h and reached a peak of 4-fold the control level at 3 h [62]. Most studies on PIPs have concentrated on responses to abiotic stress. This study offers novel insights into biological stress responses through comprehensive analysis of *MnPIPs* expression patterns under biotic stress conditions, thereby advancing our understanding of plant adaptation mechanisms.

Conclusion

In this study, 26 aquaporins were identified in mulberry trees. Bioinformatics analysis revealed that these AQPs were distributed across four subfamilies, a classification supported by phylogenetic relationships, conserved motifs, transmembrane domain characteristics, subcellular localization, and tertiary protein structure analyses. The expression profile of the *MnPIP1* subfamily genes indicated high expression levels in the roots than the *MnPIP2* subfamily genes. Furthermore, by investigating the expression profiles of in root, stem, and leaf tissues at various time points during *R. pseudosolanacearum* infection, regulatory involvement under bacterial infection was demonstrated by analyzing the expression profiles of *MnPIPs* in root, stem, and leaf tissues at various time points during infection. This study contributed to understanding the potential functions of *PIPs* in adapting to plant pathogen infections and facilitated further characterization of the identified *AQP* candidate genes in mulberry.

Materials and methods

Identification of mulberry Aquaporins gene family

The HMM model file for *AQP* genes was downloaded from the Pfam database (http://pfam.xfam.org/, accessed on 25 June 2024, Pfam accession number: PF00230), and the HMMER search was performed in the *Morus notabilis* database (https://morus.swu.edu.cn/morusdb/, accessed on 25 June 2024), with the E-value thresho ld set to 1e-5. The HMMER results were verified using the Blastp method, referencing the *Arabidopsis thaliana* database TAIR (https://www.arabidopsis.org/, accessed on 25 June 2024). After redundant sequences were removed, the candidate *AQP* gene sequences from mulberry were obtained.

Bioinformatics analysis

The physicochemical properties of the proteins were analyzed using the Protparam online tool (https://web.expasy.org/protparam/, accessed on 10 July 2024) [63]. Subc ellular localization results were predicted using PlantmPLoc 2.0 (http://www.csbio.sjtu.edu.cn/bioinf/plant-multi/, accessed on 10 July 2024) [64]. The transmembrane helices were analyzed using TMHMM (https://dtu.biolib.com/DeepTMHMM, accessed on 10 July 2024) [65], and functional domains were predicted using CDD (https://www.ncbi.nlm.nih.gov/cdd, accessed on 10 July 2024). Conserved motifs among mulberry AQPs were identified using the MEME online tool (https://meme-suite.org/meme/tools/meme, accessed on 10 July 2024) [66]. The se condary structures were predicted using SOPMA (https://npsa.lyon.inserm.fr/cgi-bin/npsa_automat.pl?page=/NPSA/npsa_sopma.html, accessed on 10 July 2024) [67], and the tertiary structures were predicted by AlphaFold2 (https://colab.research.google.com/github/sokrypton/ColabFold/blob/main/AlphaFold2.ipynb?pli=1#scrollTo=_sztQyz29DIC, accessed on 10 July 2024) [68]. The AQP sequences of *Arabidopsis thaliana*, *Vitis vinifera*, and *Camellia sinensis* used in this study were retrieved from the NCBI Protein Database (https://www.ncbi.nlm.nih.gov/protein/, accessed on 25 June 2024). Multiple sequence alignment of the amino acid sequences of mulberry aquaporin proteins was performed using ESPript 3.0 (https://espript.ibcp.fr/ESPript/ESPript/index.php, accessed on 10 July 2024) [69]. Based on the alignment results, a phylogenetic tree of AQPs amino acid sequences from *Arabidopsis*, *Camellia*, *Vitis* and *Morus* was constructed

using MEGA 11 software [70]. The Neighbor-Joining (NJ) method with a *p*-distance model was employed for the construction. Bootstrap analysis was conducted with 1000 replicates and 95% partial delection [71]. Finally, the evolutionary tree was refined using iTOL (https://itol.embl.de/itol_account.cgi, accessed on 10 July 2024) [72]. TBtools software intercepted a 2000 bp region upstream of the start codon of *MnAQP* genes as a promoter, and then the cis-acting elements are predicted through PlantCare website (http://bioinformatics.psb.ugent.be/webtools/plantcare/html/, accessed on 15 Mar 2025) [73].

Plant materials and bacterial strains

The seeds of the mulberry variety Fengchi were provided by the Mulberry Research Office of our college. The seeds were sterilized with 2% NaClO, germinated in petri dishes, and then transplanted into sterilized nutrient soil. The plants were grown under controlled conditions: 26 °C, 70% relative humidity, and 10,000 lx light for a 16 h lightness followed by 8 h of darkness. As previously mentioned, the *Nicotiana benthamiana* plants used for subcellular localization were also cultivated in the greenhouse under the same conditions. The *Ralstonia pseudosolanacearum* strain MRS-5 (GenBank: GCA_021229115.1) was used in this study, initially isolated from diseased mulberry plants located in Luogang, Guangdong Province, in our lab.

Bacterial infection

To inoculate the MRS-5 strain, a root irrigation method was used. The glycerol stock of MRS-5 was retrieved from the – 80 °C freezer, and the bacteria were streaked onto a TTC (2,3,5-triphenyltetrazolium chloride) agar plates and incubated at 28 °C for 48 h. A single colony was cultured in CPG (casamino acid–peptone–glucose) liquid medium at 28 °C with agitation at 220 rpm for 48 h. The bacteria were then suspended in sterile water and adjusted to an OD_{600} of 0.5. Mulberry seedlings were gently removed from the soil, rinsed with clean water, and inoculated into shake flasks containing 150 mL of *R. pseudosolanacearum* suspension. An equal volume of sterile water was used to inoculate a control group of seedlings (Fig. S1). Samples were collected at 0, 6, 12, 24, 48, 72 and 96 h post-inoculation. These samples were immediately frozen in liquid nitrogen and stored at -80 °C for subsequent RNA extraction.

Verification of bacterial colonization in inoculated mulberry seedling roots using Koch's postulates and electron microscopic observation of the pathogen

The roots of mulberry seedlings, collected 96 h post-inoculation with *R. pseudosolanacearum*, were subjected to surface sterilization through sequential treatment with 0.3% NaClO for 30 s and 75% ethanol for 45 s, followed by three rinses with sterile distilled water. A 100 mg sample of root tissue was placed into a grinding tube, to which 500 µL of ddH_2O was added. The tissue was ground using a plant tissue grinder. After the bacterial suspension was thoroughly mixed, it was diluted with sterile water to a concentration of 10^{-5}. 10 µL of the diluted suspension were plated on TTC solid medium. Cell slides were placed in a 12-well plate containing CPG liquid medium and bacterial suspension (OD_{600} = 0.6), followed by incubation at 28 °C for 12 h. The cell slides were fixed with 2.5% glutaraldehyde and processed for subsequent scanning electron microscopy (SEM) observation, as described in previous researches [4]. The morphological of *R. pseudosolanacearum* cells were observed using SEM (equipped with 5.00 kV EHT, SE2 signal, GeminiSEM 300, Carl Zeiss, Oberkochen, Germany).

Subcellular localization

The coding sequences (CDS) of the *MnPIP* genes, excluding the stop codon, were cloned into the *p*NC-Cam1304-SubN vector to generate the recombinant plasmids *p*NC-Cam1304-*MnPIP1;1*, *p*NC-Cam1304-*MnPIP1;2*, *p*NC-Cam1304-*MnPIP1;3*, *p*NC-Cam1304-*MnPIP2;2* and *p*NC-Cam1304-*MnPIP2;7*. Primers for plasmid construction are provided in Table S1. These recombinant plasmids were then transformed into *Agrobacterium tumefaciens* GV3101 along with the helper plasmid *p*Soup [74]. *A. tumefaciens* was cultured in Luria-Bertani liquid medium containing kanamycin, gentamycin and rifampicin at 28 °C 180 rpm until OD_{600} = 1.0. Centrifuged at 5000 rpm for 10 min to collect the bacteria, the Infiltration Buffer (1 M $MgCl_2$, 0.5 M MES, 100 mM Acetosyringone) was resuspended, and OD_{600} = 0.8 was adjusted after washing for three times, then subsequently injected into tobacco leaves. Fluorescence was observed at a wavelength of 514 nm using laser confocal microscopy (LSM880; Zeiss, Oberkochen, Germany).

Gene expression analysis

RNA was extracted from different tissues of mulberry using the RNAiso Plus reagent (Takara, Japan). The concentration and quality of the RNA were assessed using a Nanodrop 2000 spectrometer (Thermo Scientific, USA) and an Agilent Bioanalyzer 2100 (Agilent Technologies, USA). Additionally, RNA integrity was verified by 1.2% agarose gel electrophoresis (Fig. S2). The first-strand cDNA was synthesized according to the manufacturer's instructions (Yeasen, China). The primers for *MnPIPs* used in RT-qPCR were designed with Primer-BLAST (https://www.ncbi.nlm.nih.gov/tools/primer-blast/, accessed on 25 Oct 2024) [75] and synthesized by Sangon (China). These primers were listed in Table S2. The mulberry actin

gene was used as an internal reference gene [76], and the relative expression levels were calculated using the $2^{-\Delta\Delta CT}$ method [77].

Statistical analysis

All experiments were systematically repeated a minimum of three times, consistently yielding similar results. Statistical analyses were carried out using IBM Statistical Product and Service Solutions (SPSS) software, version 25. 0. A student' *t*-test was utilized to compare mean differences at a significance level. The asterisks indicate different levels of statistical significance: *, $P<0.05$; **, $P<0.01$; ***, $P<0.001$; ****, $P<0.0001$.

Supplementary Information

The online version contains supplementary material available at https://doi.org/10.1186/s12870-025-06541-7.

Supplementary Material 1

Supplementary Material 2

Supplementary Material 3

Acknowledgements

We thank Dr. Pu Yan from Institute of Tropical Biotechnology, Chinese Academy of Tropical Agricultural Sciences (ITBB, CATAS) for providing the pNC-Cam1304-SubN vector. We would like to thank Dr. Mingfeng Feng from Nanjing Agricultural University for providing guidance in subcellular localization observation. We express our gratitude to the reviewers and editors. Thank you for taking the time out of your busy schedules to review our manuscript.

Author contributions

WS: Writing – review & editing, Writing – original draft, Software, Methodology, Investigation, Data curation. DX and TQ: Resources, Methodology, Data curation. DJ and SS: Software, Methodology, Formal analysis. SH and ZW: Visualization, Data curation, Resources. LP: Writing – review & editing, Supervision, Funding acquisition, Conceptualization. All authors have read and approved the final manuscript.

Funding

This work was supported by the Natural Science Foundation of Jiangsu Province (grant number: BK20210878), Postgraduate Research & Practice Innovation Program of Jiangsu Province (grant number: SJCX24_2565), the Doctoral Starting up Foundation of Jiangsu university of Science and Technology (grant number: 1732932003), China Postdoctoral Science Foundation (grant number: 2023M742936), the Key Research and Development Program (Modern Agriculture) of Zhenjiang City (grant number: NY2024023).

Data availability

All data and materials supporting the findings of this study are available in the main article and its supplementary information files.

Declarations

Ethics approval and consent to participate

Not applicable.

Consent for publication

Not applicable.

Competing interests

The authors declare no competing interests.

Received: 14 February 2025 / Accepted: 11 April 2025
Published online: 25 April 2025

References

1. Zhou YN, Yang HY, Liu JP. Complete genome sequence of *Enterobacter roggenkampii* strain KQ-01, isolated from bacterial wilt-resistant mulberry cultivar YS283. Plant Dis. 2021;105(3):688–90.
2. Zhu PP, Zhang S, Li RL, Liu CY, Fan W, Hu TZ, Zhao AC. Host-induced gene Silencing of a G protein α subunit gene *CsGpa1* involved in pathogen appressoria formation and virulence improves tobacco resistance to *Ciboria Shiraiana*. J Fungi (Basel). 2021;7(12):1053.
3. Xuan ZY, Xie JX, Yu HD, Zhang S, Li RH, Cao MJ. Mulberry (*Morus alba*) is a new natural host of Citrus leaf blotch virus in China. Plant Dis. 2020;10.
4. Li P, Wang SY, Liu MY, Dai X, Shi HC, Zhou WH, Sheng S, Wu FA. Antibacterial activity and mechanism of three root exudates from mulberry seedlings against *Ralstonia pseudosolanacearum*. Plants (Basel). 2024;13(4):482.
5. Zhu YX, Yang L, Liu N, Yang J, Zhou XK, Xia YC, He Y, He YQ, Gong HJ, Ma DF, Yin JL. Genome-wide identification, structure characterization, and expression pattern profiling of Aquaporin gene family in cucumber. BMC Plant Biol. 2019;19(1):345.
6. Yi XF, Sun XC, Tian R, Li KX, Ni M, Ying JL, Xu L, Liu LW, Wang Y. Genome-wide characterization of the Aquaporin gene family in radish and functional analysis of *RsPIP2-6* involved in salt stress. Front Plant Sci. 2022;13:860742.
7. Chaumont F, Barrieu F, Wojcik E, Chrispeels MJ, Jung R. Aquaporins constitute a large and highly divergent protein family in maize. Plant Physiol. 2001;125(3):1206–15.
8. Wang R, Li RZ, Cheng LN, Wang XY, Fu X, Dong XF, Qi MF, Jiang CZ, Xu T, Li TL. SlERF52 regulates *SlTIP1;1* expression to accelerate tomato pedicel abscission. Plant Physiol. 2021;185(4):1829–46.
9. Danielson JA, Johanson U. Unexpected complexity of the Aquaporin gene family in the moss *Physcomitrella patens*. BMC Plant Biol. 2008;8:45.
10. Laloux T, Junqueira B, Maistriaux LC, Ahmed J, Jurkiewicz A, Chaumont F. Plant and mammal Aquaporins: same but different. Int J Mol Sci. 2018;19(2):521.
11. Johanson U, Karlsson M, Johansson I, Gustavsson S, Sjövall S, Fraysse L, Weig AR, Kjellbom P. The complete set of genes encoding major intrinsic proteins in *Arabidopsis* provides a framework for a new nomenclature for major intrinsic proteins in plants. Plant Physiol. 2001;126(4):1358–69.
12. Sakurai J, Ishikawa F, Yamaguchi T, Uemura M, Maeshima M. Identification of 33 rice Aquaporin genes and analysis of their expression and function. Plant Cell Physiol. 2005;46(9):1568–77.
13. Wong DCJ, Zhang L, Merlin I, Castellarin SD, Gambetta GA. Structure and transcriptional regulation of the major intrinsic protein gene family in grapevine. BMC Genomics. 2018;19(1):248.
14. Gupta AB, Sankararamakrishnan R. Genome-wide analysis of major intrinsic proteins in the tree plant *Populus trichocarpa*: characterization of XIP subfamily of Aquaporins from evolutionary perspective. BMC Plant Biol. 2009;9:134.
15. Park W, Scheffler BE, Bauer PJ, Campbell BT. Identification of the family of Aquaporin genes and their expression in upland cotton (*Gossypium hirsutum* L). BMC Plant Biol. 2010;10:142.
16. He NJ, Zhang C, Qi XW, Zhao SC, Tao Y, Yang GJ, Lee TH, Wang XY, Cai QL, Li D, Lu MZ, Liao ST, Luo GQ, He RJ, Tan X, Xu YM, Li T, Zhao AC, Jia L, Fu Q, Zeng QW, Gao C, Ma B, Liang JB, Wang XL, Shang JZ, Song PH, Wu HY, Fan L, Wang Q, Shuai Q, Zhu JJ, Wei CJ, Zhu-Salzman KY, Jin DC, Wang JP, Liu T, Yu MD, Tang CM, Wang ZJ, Dai FW, Chen JF, Liu Y, Zhao ST, Lin TB, Zhang SG, Wang JY, Wang J, Yang HM, Yang GW, Wang J, Paterson AH, Xia QY, Ji DF, Xiang ZH. Draft genome sequence of the mulberry tree *Morus notabilis*. Nat Commun. 2013;4:2445.
17. Singh RK, Deshmukh R, Muthamilarasan M, Rani R, Prasad M. Versatile roles of Aquaporin in physiological processes and stress tolerance in plants. Plant Physiol Biochem. 2020;149:178–89.
18. Genin S. Molecular traits controlling host range and adaptation to plants in *Ralstonia solanacearum*. New Phytol. 2010;187(4):920–8.
19. Xue H, Lozano-Durán R, Macho AP. Insights into the root invasion by the plant pathogenic bacterium *Ralstonia solanacearum*. Plants (Basel). 2020;9(4):516.
20. Inoue K, Takemura C, Senuma W, Maeda H, Kai K, Kiba A, Ohnishi K, Tsuzuki M, Hikichi Y. The behavior of *Ralstonia pseudosolanacearum* strain OE1-1 and morphological changes of cells in tomato roots. J Plant Res. 2023;136(1):19–31.

21. Wang ZJ, Luo WB, Cheng SJ, Zhang HJ, Zong J, Zhang Z. *Ralstonia solanacearum* - A soil borne hidden enemy of plants: research development in management strategies, their action mechanism and challenges. Front Plant Sci. 2023;14:1141902.
22. Wang CM, Song BB, Dai YQ, Zhang SL, Huang XS. Genome-wide identification and functional analysis of U-box E3 ubiquitin ligases gene family related to drought stress response in Chinese white Pear (*Pyrus bretschneideri*). BMC Plant Biol. 2021;21(1):235.
23. Zhang YH, Zhao XF, Li B, Liu C, Yu XM, Zhang ZD, Zhang SH, Li JM. Plasma membrane intrinsic proteins *SlPIP2;5* gene regulates tolerance to high VPD in tomato. Environ Exp Bot. 2024;222:105771.
24. Sohail H, Noor I, Nawaz MA, Ma MR, Shireen F, Huang Y, Yang L, Bie ZL. Genome-wide identification of plasma-membrane intrinsic proteins in pumpkin and functional characterization of *CmoPIP1-4* under salinity stress. Environ Exp Bot. 2022;202:104995.
25. He YL, Chen YY, Zhang YW, Qin XF, Wei XL, Zheng DH, Lin W, Li QQ, Y GQ. Genetic diversity of *Ralstonia solanacearum* species complex strains obtained from Guangxi, China and their pathogenicity on plants in the Cucurbitaceae family and other botanical families. Plant Pathol. 2021;70(6):1445–54.
26. Zhang M, Shi HT, Li NN, Wei NN, Tian Y, Peng JF, Chen XC, Zhang LY, Zhang MX, Dong HS. Aquaporin OsPIP2;2 links the H_2O_2 signal and a membrane-anchored transcription factor to promote plant defense. Plant Physiol. 2022;188(4):2325–41.
27. Ai G, Xia QY, Song TQ, Li TL, Zhu H, Peng H, Liu J, Fu XW, Zhang M, Jing MF, Xia A, Dou DL. A *Phytophthora Sojae* CRN effector mediates phosphorylation and degradation of plant Aquaporin proteins to suppress host immune signaling. PLoS Pathog. 2021;17(3):e1009388.
28. Zhang H, Yang ZT, Cheng GY, Luo TX, Zeng K, Jiao WD, Zhou YS, Huang GQ, Zhang JS, Xu JS. *Sugarcane mosaic virus* employs 6K2 protein to impair ScPIP2;4 transport of H_2O_2 to facilitate virus infection. Plant Physiol. 2024;194(2):715–31.
29. Yadav E, Yadav N, Hus A, Yadav JS. Aquaporins in lung health and disease: emerging roles, regulation, and clinical implications. Respir Med. 2020;174:106193.
30. Chaumont F, Moshelion M, Daniels MJ. Regulation of plant Aquaporin activity. Biol Cell. 2005;97(10):749–64.
31. Shivaraj SM, Deshmukh RK, Rai R, Bélanger R, Agrawal PK, Dash PK. Genome-wide identification, characterization, and expression profile of Aquaporin gene family in flax (*Linum usitatissimum*). Sci Rep. 2017;7:46137.
32. Salvatierra A, Mateluna P, Toro G, Solís S, Pimentel P. Genome-wide identification and gene expression analysis of sweet Cherry Aquaporins (*Prunus avium* L.) under abiotic stresses. Genes (Basel). 2023;14(4):940.
33. Inden T, Hoshino A, Otagaki S, Matsumoto S, Shiratake K. Genome-wide analysis of Aquaporins in Japanese morning glory (*Ipomoea nil*). Plants (Basel). 2023;12(7):1511.
34. Zou Z, Zheng YJ, Chang LL, Zou LP, Zhang L, Min Y, Zhao YG. TIP Aquaporins in *Cyperus esculentus*: genome-wide identification, expression profiles, subcellular localizations, and interaction patterns. BMC Plant Biol. 2024;24(1):298.
35. Kong WL, Bendahmane M, Fu XP. Genome-wide identification and characterization of Aquaporins and their role in the flower opening processes in carnation (*Dianthus caryophyllus*). Molecules. 2018;23(8):1895.
36. Venisse JS, Õunapuu-Pikas E, Dupont M, Gousset-Dupont A, Saadaoui M, Faize M, Chen S, Chen S, Petel G, Fumanal B, Roeckel-Drevet P, Sellin A, Label P. Genome-wide identification, structure characterization, and expression pattern profiling of the Aquaporin gene family in *Betula pendula*. Int J Mol Sci. 2021;22(14):7269.
37. Quigley F, Rosenberg JM, Shachar-Hill Y, Bohnert HJ. From genome to function: the *Arabidopsis* Aquaporins. Genome Biol. 2002;3(1):RESEARCH0001.
38. Tayade R, Rana V, Shafiqul M, Nabi RBS, Raturi G, Dhar H, Thakral V, Kim Y. Genome-wide identification of Aquaporin genes in Adzuki bean (*Vigna angularis*) and expression analysis under drought stress. Int J Mol Sci. 2022;23(24):16189.
39. Shelden MC, Howitt SM, Kaiser BN, Tyerman SD. Identification and functional characterisation of Aquaporins in the grapevine, *Vitis vinifera*. Funct Plant Biol. 2010;36(12):1065–78.
40. Ma B, Wang HH, Liu JC, Chen L, Xia XY, Wei WQ, Yang Z, Yuan JL, Luo YW, He NJ. The gap-free genome of mulberry elucidates the architecture and evolution of polycentric chromosomes. Hortic Res. 2023;10(7):uhad111.
41. Zeng QX, Jia HF, Ma YY, Xu LW, Ming R, Yue JJ. Genome-wide identification and expression pattern profiling of the Aquaporin gene family in Papaya (*Carica Papaya* L). Int J Mol Sci. 2023;24(24):17276.
42. Chaumont F, Tyerman SD. Aquaporins: highly regulated channels controlling plant water relations. Plant Physiol. 2014;164(4):1600–18.
43. Kaldenhoff R, Ribas-Carbo M, Sans JF, Lovisolo C, Heckwolf M, Uehlein N. Aquaporins and plant water balance. Plant Cell Environ. 2008;31(5):658–66.
44. Maurel C, Verdoucq L, Luu DT, Santoni V. Plant Aquaporins: membrane channels with multiple integrated functions. Annu Rev Plant Biol. 2008;59:595–624.
45. Hachez C, Besserer A, Chevalier AS, Chaumont F. Insights into plant plasma membrane Aquaporin trafficking. Trends Plant Sci. 2013;18(6):344–52.
46. Zhang LY, Chen L, Dong HS. Plant Aquaporins in infection by and immunity against pathogens - a critical review. Front Plant Sci. 2019;10:632.
47. Li GJ, Chen T, Zhang ZQ, Li BQ, Tian SP. Roles of Aquaporins in plant-pathogen interaction. Plants (Basel). 2020;9(9):1134.
48. Gómez-Méndez MF, Amezcua-Romero JC, Rosas-Santiago P, Hernández-Domínguez EE, de Luna-Valdez LA, Ruiz-Salas JL, Vera-Estrella R, Pantoja O. Ice plant root plasma membrane Aquaporins are regulated by clathrin-coated vesicles in response to salt stress. Plant Physiol. 2023;191(1):199–218.
49. Bai JQ, Wang X, Yao XH, Chen XC, Lu K, Hu YQ, Wang ZD, Mu YJ, Zhang LY, Dong HS. Rice Aquaporin OsPIP2;2 is a water-transporting facilitator in relevance to drought-tolerant responses. Plant Direct. 2021;5(8):e338.
50. Li P, Zhang LY, Mo XY, Ji HT, Bian HJ, Hu YQ, Majid T, Long JY, Pang H, Tao Y, Ma JB, Dong HS. Rice Aquaporin PIP1;3 and Harpin Hpa1 of bacterial blight pathogen cooperate in a type III effector translocation. J Exp Bot. 2019;70(12):3057–73.
51. Yao XH, Mu YJ, Zhang LY, Chen L, Zou SS, Chen XC, Lu K, Dong HS. AtPIP1;4 and AtPIP2;4 cooperatively mediate H_2O_2 transport to regulate plant growth and disease resistance. Plants (Basel). 2024;13(7):1018.
52. Sun YB, Ren XY, Guo WH, Wang Y, Yan H, Han LR, Feng JT. Protein elicitor GP1pro targets Aquaporin NbPIP2;4 to activate plant immunity. Plant Cell Environ. 2023;46(8):2575–89.
53. Yu XS, Wang HR, Lei FF, Li RQ, Yao HP, Shen JB, Ain NU, Cai Y. Structure and functional divergence of PIP peptide family revealed by functional studies on PIP1 and PIP2 in *Arabidopsis thaliana*. Front Plant Sci. 2023;14:1208549.
54. Zhou L, Xiang XQ, Ji DP, Chen QL, Ma TF, Wang JG, Liu CX. A carbonic anhydrase, ZmCA4, contributes to photosynthetic efficiency and modulates CO_2 signaling gene expression by interacting with Aquaporin ZmPIP2;6 in maize. Plant Cell Physiol. 2024;65(2):243–58.
55. Yue C, Cao HL, Wang L, Zhou YH, Hao XY, Zeng JM, Wang XC, Yang YJ. Molecular cloning and expression analysis of tea plant Aquaporin (AQP) gene family. Plant Physiol Biochem. 2014;83:65–76.
56. Hachez C, Moshelion M, Zelazny E, Cavez D, Chaumont F. Localization and quantification of plasma membrane Aquaporin expression in maize primary root: a clue to Understanding their role as cellular plumbers. Plant Mol Biol. 2006;62(1–2):305–23.
57. Suga S, Murai M, Kuwagata T, Maeshima M. Differences in Aquaporin levels among cell types of radish and measurement of osmotic water permeability of individual protoplasts. Plant Cell Physiol. 2003;44(3):277–86.
58. Javot H, Lauvergeat V, Santoni V, Martin-Laurent F, Güçlü J, Vinh J, Heyes J, Franck KI, Schäffner AR, Bouchez D, Maurel C. Role of a single Aquaporin isoform in root water uptake. Plant Cell. 2003;15(2):509–22.
59. Zelazny E, Borst JW, Muylaert M, Batoko H, Hemminga MA, Chaumont F. FRET imaging in living maize cells reveals that plasma membrane Aquaporins interact to regulate their subcellular localization. Proc Natl Acad Sci U S A. 2007;104(30):12359–64.
60. Chaumont F, Barrieu F, Jung R, Chrispeels MJ. Plasma membrane intrinsic proteins from maize cluster in two sequence subgroups with differential Aquaporin activity. Plant Physiol. 2000;122(4):1025–34.
61. Wang XB, Lu K, Yao XH, Zhang LY, Wang FB, Wu DG, Peng JF, Chen XC, Du JL, Wei JK, Ma JY, Chen L, Zou SS, Zhang CL, Zhang MX, Dong HS. The Aquaporin TaPIP2;10 confers resistance to two fungal diseases in wheat. Phytopathology. 2021;111(12):2317–31.
62. Yin YX, Wang SB, Zhang HX, Xiao HJ, Jin JH, Ji JJ, Jing H, Chen RG, Arisha MH, Gong ZH. Cloning and expression analysis of *CaPIP1-1* gene in pepper (*Capsicum annuum* L). Gene. 2015;563(1):87–93.
63. Gasteiger E, Gattiker A, Hoogland C, Ivanyi I, Appel RD, Bairoch A. ExPASy: the proteomics server for in-depth protein knowledge and analysis. Nucleic Acids Res. 2003;31(13):3784–8.
64. Chou KC, Shen HB. Cell-PLoc: a package of web servers for predicting subcellular localization of proteins in various organisms. Nat Protoc. 2008;3(2):153–62.

65. Kahsay RY, Gao G, Liao L. An improved hidden Markov model for transmembrane protein detection and topology prediction and its applications to complete genomes. Bioinformatics. 2005;21(9):1853–8.
66. Bailey TL, Boden M, Buske FA, Frith M, Grant CE, Clementi L, Ren J, Li WW, Noble WS. MEME SUITE: tools for motif discovery and searching. Nucleic Acids Res. 2009;37(Web Server issue):W202–8.
67. Geourjon C, Deléage G. SOPMA: significant improvements in protein secondary structure prediction by consensus prediction from multiple alignments. Comput Appl Biosci. 1995;11(6):681–4.
68. Kim G, Lee S, Levy Karin E, Kim H, Moriwaki Y, Ovchinnikov S, Steinegger M, Mirdita M. Easy and accurate protein structure prediction using ColabFold. Nat Protoc. 2025;20(3):620–42.
69. Robert X, Gouet P. Deciphering key features in protein structures with the new endscript server. Nucleic Acids Res. 2014;42(Web Server issue):W320–4.
70. Tamura K, Stecher G, Kumar S. MEGA11: molecular evolutionary genetics analysis version 11. Mol Biol Evol. 2021;38(7):3022–7.
71. Kumar S, Stecher G, Li M, Knyaz C, Tamura K. MEGA X: molecular evolutionary genetics analysis across computing platforms. Mol Biol Evol. 2018;35(6):1547–9.
72. Letunic I, Bork P. Interactive tree of life (iTOL) v5: an online tool for phylogenetic tree display and annotation. Nucleic Acids Res. 2021;49(W1):W293–6.
73. Luo SL, Zhang GB, Zhang ZY, Wan ZL, Liu ZC, Lv J, Yu JH. Genome-wide identification and expression analysis of *BZR* gene family and associated responses to abiotic stresses in cucumber (*Cucumis sativus* L). BMC Plant Biol. 2023;23(1):214.
74. Yan P, Tuo DC, Shen WT, Deng HD, Zhou P, Gao XZ. A nimble cloning-compatible vector system for high-throughput gene functional analysis in plants. Plant Commun. 2023;4(2):100471.
75. Ye J, Coulouris G, Zaretskaya I, Cutcutache I, Rozen S, Madden TL. Primer-BLAST: a tool to design target-specific primers for polymerase chain reaction. BMC Bioinformatics. 2012;13:134.
76. Pan G, Lou CF. Isolation of an 1-aminocyclopropane-1-carboxylate oxidase gene from mulberry (*Morus Alba* L.) and analysis of the function of this gene in plant development and stresses response. J Plant Physiol. 2008;165(11):1204–13.
77. Livak KJ, Schmittgen TD. Analysis of relative gene expression data using real-time quantitative PCR and the 2(-Delta Delta C(T)) method. Methods. 2001;25(4):402–8.

Publisher's note